Supplementary Information

A novel core-shell nanoclusters composed of multiple Nickel-Cobalt-OxySelenide nanowires wrapped with NiCo-LDH nanosheets for high energy density hybrid supercapacitors

Runmei Luo, Qingjun Yang, Yu Liu, Lin Sun, Changhong Wang, Min Chen* and Weidong Shi*.

School of Chemistry and Chemical Engineering, Jiangsu University, Zhenjiang 212013, PR China.

**Corresponding Author*

E-mail: swd1978@ujs.edu.cn; Tel: +86-511-88791800

***Characterization*:** The instrument used for XRD testing is the D/max-2500 powder X-ray diffractometer, which identifies the range from 5° to 80° at 5°/min within 2θ, XPS mode (Thermo ESCALAB 250 x) to identify atomic valence information, transmission electron microscopy (TEM, F 20 S-TWIN Tecnai G 2, FEI Co. 200 kV) and scanning electron microscope (SEM, Hitachi S-4800, Japan) to characterize the structures.

Electrochemical measurement: The CHI 660 electrochemical workstation (Hua Chen, Shanghai, China) was to be used to check the electrochemical properties of almost all electrode materials in a 6 M KOH electrolyte solution. Cyclic voltammetry, constant current charge/discharge, and electrochemical impedance performance tests were conducted using conventional three electrodes, consisting of a sheet of platinum as a counter electrode and Hg/HgO reference and working electrodes (the immersion area was kept at 1 cm^2). The positive and negative electrodes of an asymmetric supercapacitor made of NCOSe/Ni_2Co_1-LDH were put together. The mass load of negative material (Δm), the specific capacity of two electrode configurations, the energy density (E) of the HSC device, and the power density (P) were all computed using the charge balance of the positive and negative electrodes:

$$\frac{m+}{m-} = \frac{C- \times V-}{C+ \times V+} \quad (1)$$

$$C = \frac{I \times \Delta t}{M} \quad (2)$$

$$E = \frac{I \int V dt}{M \times 3.6} \quad (3)$$

$$P = \frac{E \times 3600}{\Delta t} \quad (4)$$

C_{s+} (F g^{-1}) represents NCOSe/Ni_2Co_1-LDH, C_{s-} (F g^{-1}) represents the specific capacity of AC, V_+, V_- respectively voltage windows of the anode and cathode, Δ t stands for the discharge time (s), I represents the drain current (A), M represents the load mass (g) of the positive and negative electrodes, and V shows the potential window of the discharge process.

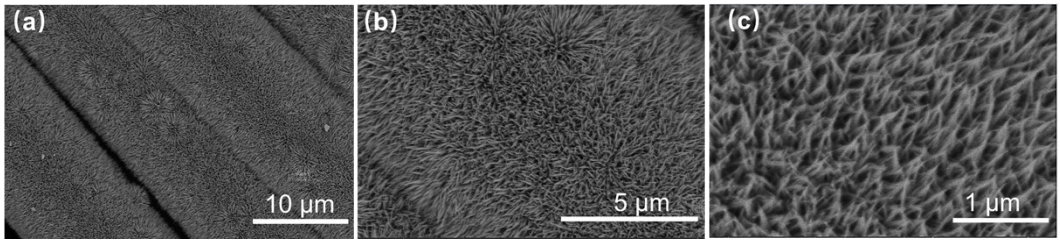

Fig. S1 SEM patterns of NiCo-CH

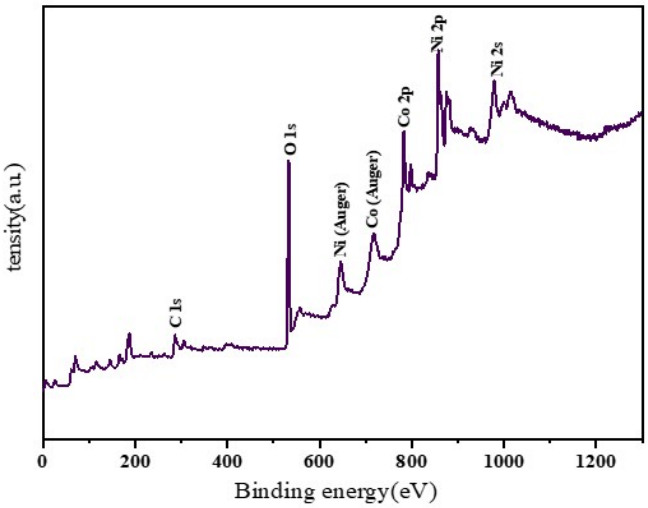

Fig. S2 XPS survey spectrum of NCOSe/Ni_2Co_1-LDH

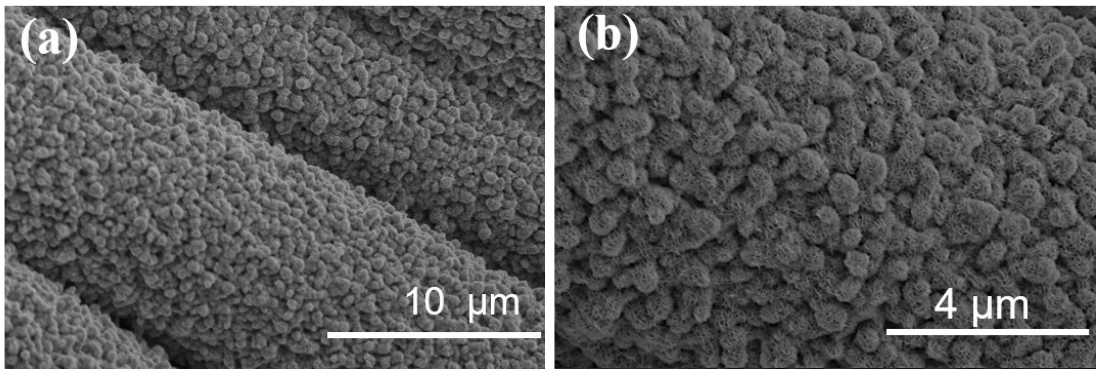

Fig. S3 SEM patterns of nanocluster NCOSe/Ni_2Co_1-LDH

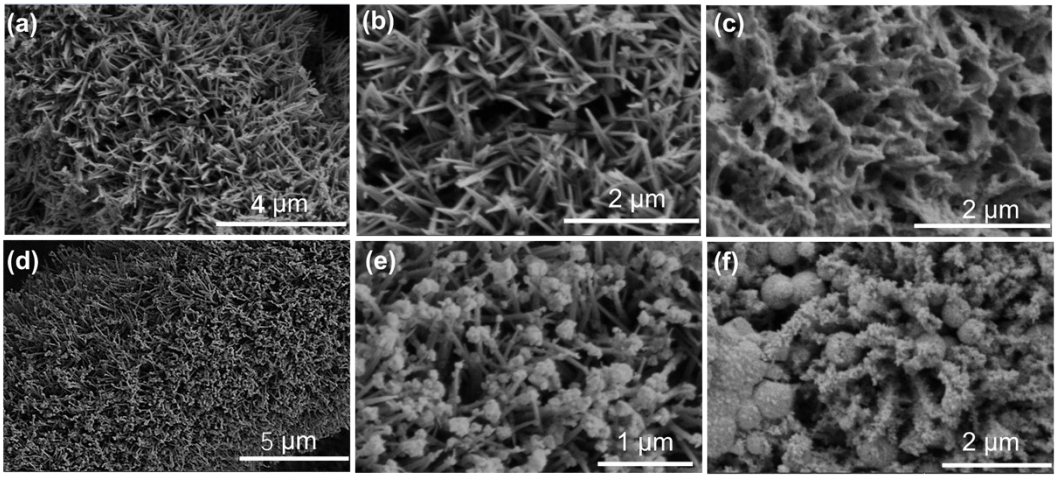

Fig. S4. The SEM images of Ni_1Co_2-CH NAs (a-b), N_1C_2OSe-8 NAs (c), Ni_2Co_1-CH NAs (d-e), and N_2C_1OSe-8 NAs (f).

From SEM, the distribution of Ni_1Co_2-CH nanowires is staggered and disordered, and their arrangement is not as neat and orderly as that of NiCo-CH (Fig. S4(a-b)). When Ni_1Co_2-CH is hydrothermally selenized, the nanowire surface is wrapped by thick crystals, which may result in insufficient voids to facilitate the diffusion of electrolyte ions (Fig. S4c). Fig. S4(d-e) shows that tiny crystals are distributed on the top of the Ni_2Co_1-CH nanowires, and the crystal stacking and aggregation effects are more obvious when the selenization treatment is performed, which may lead to more severe interlayer stacking in later electrodeposited LDH (Fig. S4f). Through the

above analysis, only NiCo-CH can be used as the best precursor.

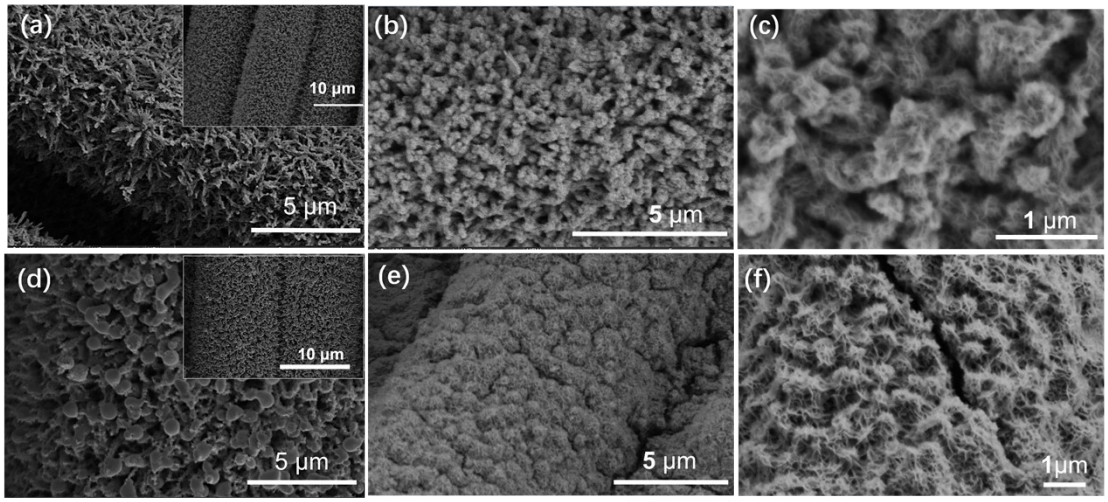

Fig. S5. The SEM images of NCOSe-6(a), NCOSe-6/Ni_2Co_1-LDH(b-c), NCOSe-10(d), and NCOSe-10/Ni_2Co_1-LDH(e-f).

When selenization was done after 6 h, selenide rarely adhered to the nanowires (Fig. S5(a)). And when the selenization was excessive after 10 h, leading to the present situation that the selenides started to agglomerate and accumulate (Fig. S5d). Then, we electrodeposited NiCo-LDH according to different selenization times, and during the electrodeposition process, two-dimensional nanosheets grew on the surface of the active nanowires of NCOSe-6 as small nanocluster structures (Fig. S5(b-c)). Similarly, the electrodeposition of LDH, at 10 h of selenization, leads to the phenomenon of faulting. This is because selenization leads to a rapid increase in the nucleation sites for electrodeposition, and the rapid adsorption of Ni^{2+} and Co^{2+} in the solution makes it favorable for the deposition of nanosheets, which eventually leads to the accumulation and stacking of nanosheets when the nanowires are not enough to support the nanosheets, which will lead to the breakage of the nanowires and the subsequent fracture of the nanosheets (Fig. S5(e-f)). On the contrary, at selenization 8h, the nanoclusters are larger at this

time and the shape remains intact. Therefore, the morphology at 8 h selenization is the most favorable for LDH growth.

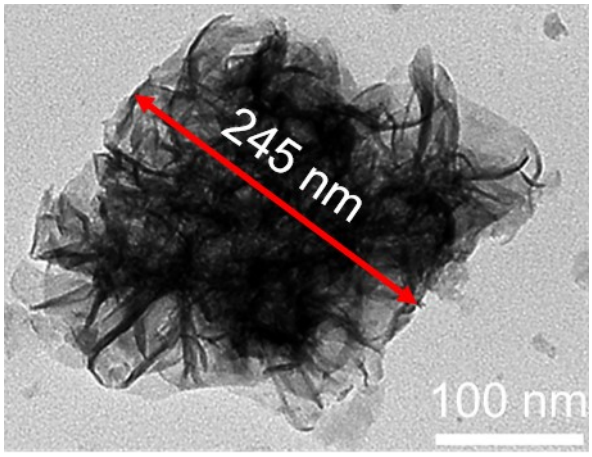

Fig. S6 STEM patterns of nanocluster NCOSe/Ni_2Co_1-LDH

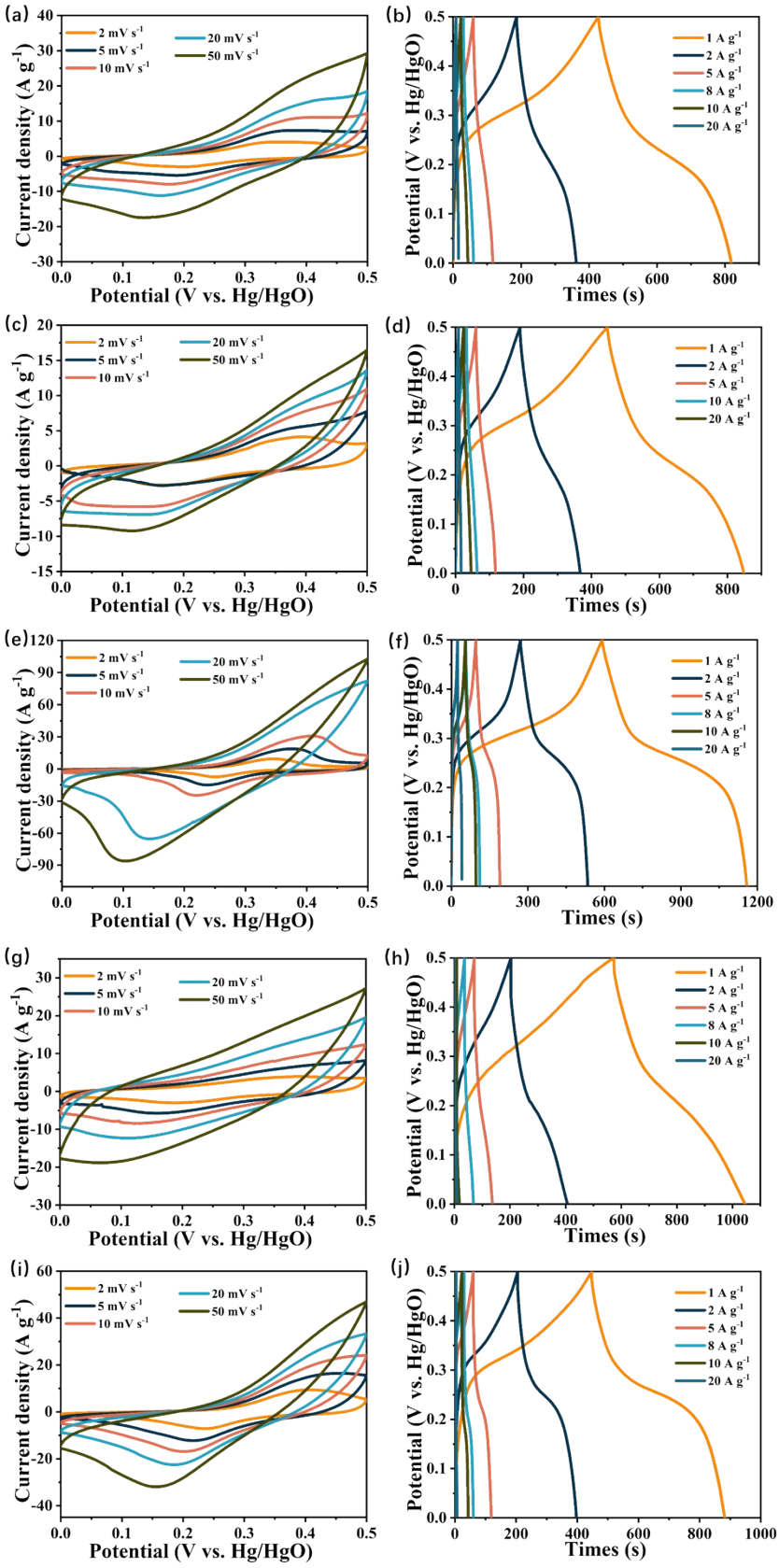

Fig. S7 (a-b) CV and GCD curves of NCOSe-4. (c-d) CV and GCD curves of NCOSe-6. (e-f) CV and GCD curves of NCOSe-8. (g-h) CV and GCD curves of NCOSe-10. (i-j) CV and GCD curves of

$(Ni,Co)_2Se$.

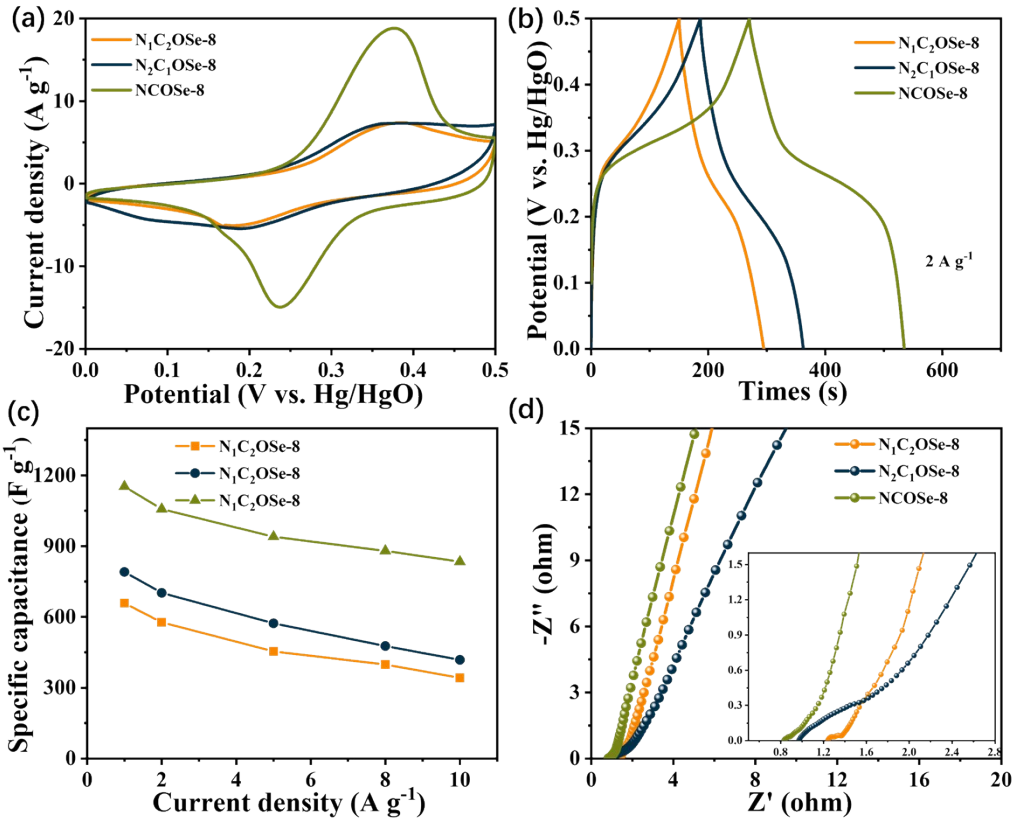

Fig. S8 (a-b) CV and GCD curves of N_2C_1OSe-8, N_1C_2OSe-8, and NCOSe-8. (c-d) Comparison of specific capacity and Nyquist plots of Ni_xCo_yOSe-8 at various current densities.

The GCD tests for NCOSe-8, N_2C_1OSe-8, and N_1C_2OSe-8 at a current density of 1 A g^{-1} found that NCOSe-8 had the longest discharge time and the largest discharge area, indicating the highest specific capacity and the smallest resistance (Fig. 8), indicating that the Ni:Co=1:1 precursor (NiCo-CH) is the most favorable for selenium chemical growth. The above is the effect of Ni and Co ratio on NCOSe.

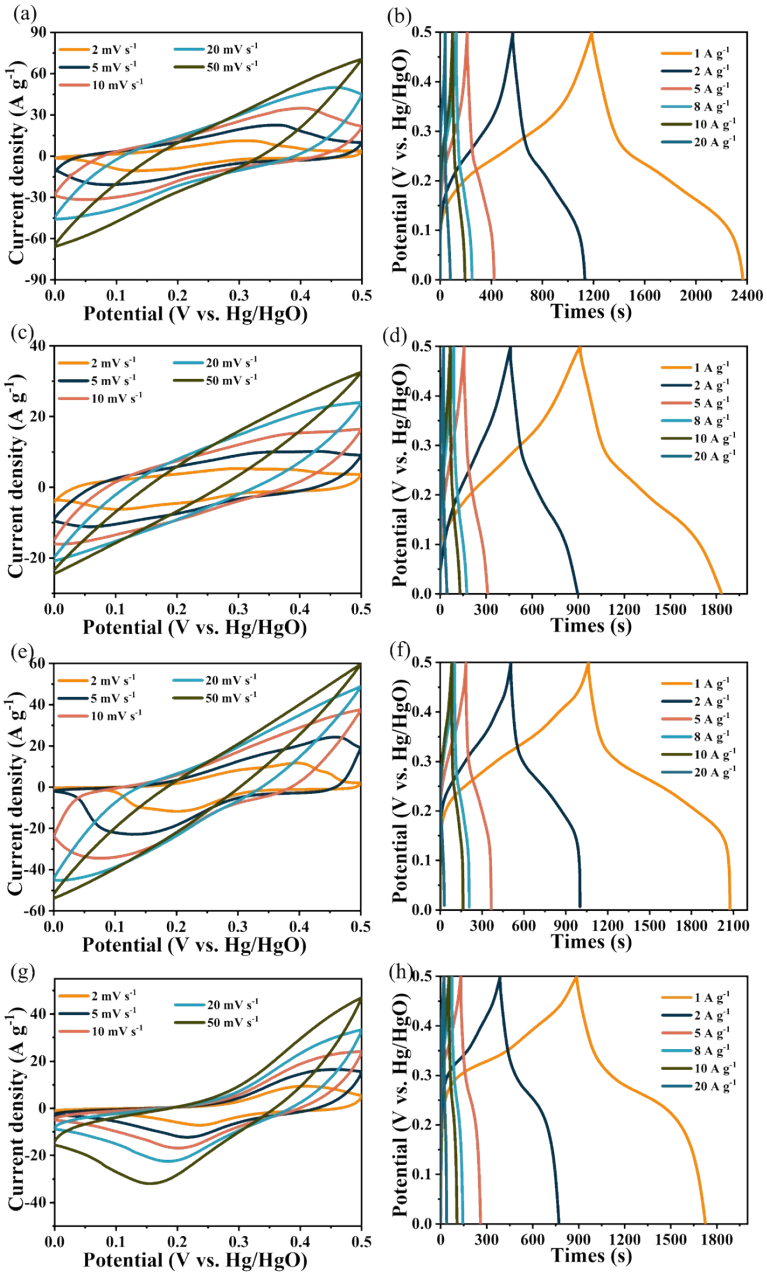

Fig. S9 (a-b) CV and GCD curves of NCOSe/Ni_1Co_1-LDH. (c-d) CV and GCD curves of NCOSe/Ni_1Co_2-LDH. (e-f) CV and GCD curves of CF@Ni_2Co_1-LDH. (g-h) CV and GCD curves of CF@Ni_3Co_1-LDH.

Table S1. The EIS fitted data for all the EIS graphs.

Sample	NCOSe-	NCOSe/Ni_2Co_1-LDH	NCOSe/Ni_1Co_1-LDH	NCOSe/Ni_1Co_2-LDH	NCOSe/Ni_3Co_1-LDH
R_s (ohm)	1.21	0.75	1.08	1.13	1.38

R_{ct} (ohm)	0.83	0.12	0.058	0.76	0.95

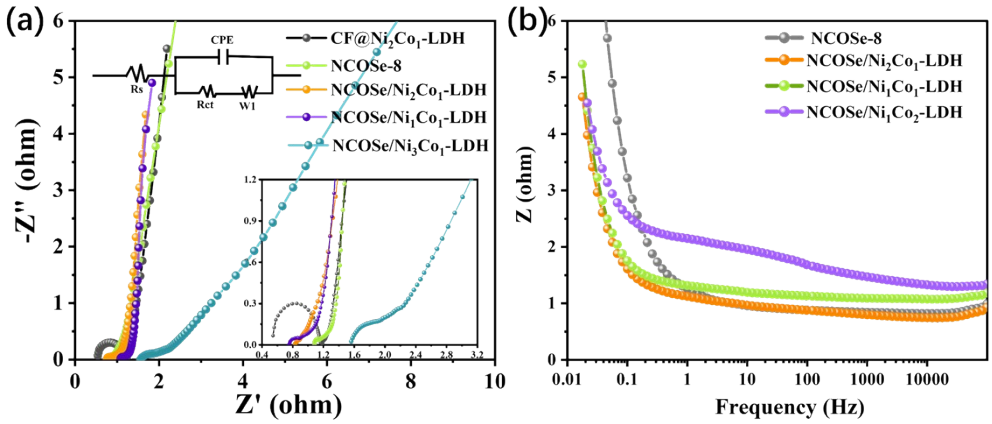

Fig. S10. (a) Nyquist plots of the electrodes CF@Ni_2Co_1-LDH, NCOSe-8, and NCOSe-/Ni_xCo_y-LDH. (b) the relationship between Z and frequency.

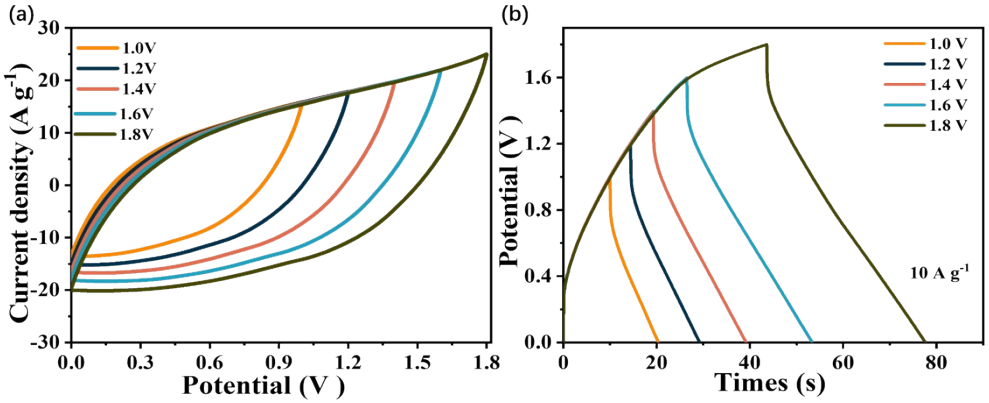

Fig. S11 (a) The HSC device's CV and (b) GCD curves at varied voltage windows.